



Fatigue strength evaluation and fracture behavior of joined dual phase steel/AA6061-T6 aluminum alloy

Celso Eduardo Cruz Gonzalez

CIDESI Estado de México. Av. Desarrollo s/n, Parque Industrial Cuamatla, 54763 Cuautitlán Izcalli, Mexico.
ecruz@cidesi.edu.mx, <http://orcid.org/0000-0001-7620-9052>

Ruben Perez Mora

CONACYT - CENTA. Carr. Est. 200 Km 23, Parque Aeroespacial Queretaro, Colón, Qro, Mexico.
ruben.perez@cidesi.edu.mx, <https://orcid.org/0000-0002-3663-8001>

Saul Daniel Santillan Gutierrez

Centro de Alta Tecnología, Universidad Autónoma Nacional de México, campus Juriquilla, Qro, Mexico.
saulsan@unam.mx, <http://orcid.org/0000-0003-2556-1640>

Jose Jaime Taha-Tijerina

Universidad de Monterrey, Departamento de Ingeniería, San Pedro Garza García, N.L., México, METALSA Technology Department, Parque de Investigación e Innovación Tecnológica (PIIT), Apodaca, N.L., Mexico
jose.taha@metalsa.com, <https://orcid.org/0000-0001-6781-9414>.

Benjamin Vargas Arista

Tecnológico Nacional de México, Instituto Tecnológico de Tlalnepantla, División de Estudios de Posgrado e Investigación, Av. Instituto Tecnológico s/n, Col. La Comunidad, Tlalnepantla de Baz, Estado de Méx., Mexico.
benvargasa@gmail.com, <http://orcid.org/0000-0002-8210-9186>

Arturo Barba Pingarron

Centro de Ingeniería de Superficies y Acabados (CENISA), Departamento de Ingeniería de Diseño y Manufactura. División de Ingeniería Mecánica e Industrial, Ciudad Universitaria, CDMX, Mexico
arbapin5@gmail.com, <http://orcid.org/0000-0001-7285-9429>.

ABSTRACT. The fatigue strength evaluation and fracture behavior for a dual phase steel-AA6061-T6 bonded joints with three different adhesives (DC-80, Betamate 120 and MP55420) are presented in this paper. Single lap shear tests were used to determine maximum shear loads, for the single lap shear testing for 5.0 mm overlap length were 2 to 3.5 times higher in comparison to the 12.7 mm overlap length specimens. The results for the strain measurement revealed that higher strain-stress were developed in the 6061-T6 aluminum alloy adherend and in all cases they were lower than the adherends yield strength. Fatigue testing was carried out at 30, 50 and 70 % of the maximum shear load, 0.1 of reversibility load ratio (R) and 30 Hz of frequency. After



Citation: Cruz Gonzalez, C.E., Perez Mora, R., Santillan Gutierrez, S., Taha-Tijerina, J., Vargas Arista, B., Barba Pingarron, A., Fatigue strength evaluation and fracture behavior of joined dual phase steel/AA6061-T6 aluminum alloy, *Frattura ed Integrità Strutturale*, 48 (2019) 530-544.

Received: 29.01.2019
Accepted: 27.02.2019



testing, Basquin and Wholer graphs were built for each adhesive at 12.7 and 50.0 mm of overlap length. The results suggested that at higher overlapping, the cyclic maximum load increased. Additionally, the maximum fatigue loading at 10^6 cycles for MP55420 adhesive was 1.3 kN for an overlapping of 12.7 mm and 2.9 kN for 50 mm. For DC80 adhesive was 1.75 kN for overlapping 12.7 mm and 4.8 kN for 50 mm. Finally, for the Betamate 120 adhesive was 1.8 kN for 12.7 mm of overlapping and 6 kN for 50 mm. The post-fracture visual inspection revealed that MP55420 and Betamate 120 adhesives had a cohesive failure, while the DC-80 showed cohesive-adhesive failure. Additionally, the scanning electron microscopy evaluation on the spew fillet revealed resolved striations and a network of small micro-dimples for the Betamate 120 and MP55420 adhesives. On the other hand, DC-80 adhesive exhibited notable facet fragile failure that was confirmed by the shape of stress-strain plot with straight line from the origin to the point of fracture.

Published: 01.04.2019

Copyright: © 2019 This is an open access article under the terms of the CC-BY 4.0, which permits unrestricted use, distribution, and reproduction in any medium, provided the original author and source are credited.

KEYWORDS. Fatigue; Overlap length; Adhesive joint strength.

INTRODUCTION

The application of adhesively bonded joints in automotive and aeronautical industries has increased significantly in recent years, having several procedures to join metals, polymers and composites by using adhesives [1]. An adhesive distributes stresses more evenly than riveted and screwed joints, thus avoiding areas of high stress concentration. Additionally, adhesive bonding allows to generate joints without microstructural changes on the parts joined, distortion, design flexibility, joining of dissimilar or new materials and good fatigue strength [2]. Joining dissimilar materials such as fiber-reinforced composites to metals or novel materials, has a goal of generating lightweight structures for decreasing fuel consumption, CO₂ emissions, among others, in transportation sector. In this sense, materials like polymer matrix composites, aluminum, magnesium or high strength steels (HSS) (< 0.5 mm thick sheets) become an alternative.

A single type material in structure is rarely realistic, because its employment depends basically on the maximum stress (and its orientation) that the structure can withstand. Even if metals cannot be excluded as fundamental base material from many applications, plastic materials are used because their low weight (2.7 or 7.8 times lighter than aluminum or steel, respectively), high corrosion resistance, excellent formability and greater design flexibility [3].

Fatigue is undoubtedly a very important type of loading for many structural components that contain adhesive bonding systems. Under fatigue loading stress, a structure may fail far below of its static strength [4]. The time that the material remains in service before the failure occurs is determined by the level of stresses and the frequency of the load cycles. The analysis is carried out by obtaining the stress-number of cycles curves (S-N) until the failure of the component occurs. The above allow an estimation of the fatigue resistance of a given material or structure [5].

Fatigue is important for reliability and durability of materials and structures, such as car or plane frames. The effect of joint geometry has been studied in order to determine its effect in the fatigue strength. An example of that is the work published by Altan et al [6], where the results suggest that fatigue strengths of adhesively-bonded butterfly joints have a longer life span than those of the bonded butt joints under the same circumstances.

Fessel et al [7] have investigated the effect of a reverse-bent joint geometry for the improvement of fatigue performance of adhesively bonded joints. The results suggest, that the improvements obtained under static tests conditions can be translated to even higher benefits in fatigue.

The effect of a highly-toughened epoxy adhesive bond-line thickness (130 to 790 μm), on the fatigue strength of 12.7 mm thick AA6061-T651 adherends has been investigated by Azari et al [8]. The experiments consisted in a double cantilever beam (DCB) and asymmetric double cantilever beam (ADCB) specimens with a surface finishing ($R_a = 1.33 \pm 0.16 \mu\text{m}$) prepared by using a silicon carbide nylon mesh. The results suggest, that the critical strain energy release rate for quasi-static fracture increased linearly with aforementioned bond-line thickness.



Adhesives exhibit a large amount of plasticity that has an important impact on the fatigue strength of adhesive joints. In that sense, Markolefas and Papathanassiou [9] proposed a shear-lag model to evaluate stress redistributions in double-lap joints under axial (tensile) lap shear cyclic loading. In this work, a double lap shear specimen model was exposed to develop stress-strain equations, then equations that governs adhesive shear stress redistributions under cyclic loading was developed. Example solutions that considers metal to metal and composite to metal were exposed. The materials, like 7076-T6 aluminum alloy (Young Modulus=71 GPa, Poisson ratio=0.33, Maximum strength=482.50 MPa and 2 mm thick), high strength graphite-epoxy composites (Young Modulus=55.15 GPa, Inter-laminar strength=55.15MPa, Maximum strength=475.69 MPa and 1.5 mm thick) and Hysol Shell EA951 adhesive (Shear Modulus=415.67 MPa, Young Modulus=3.447 GPa, Shear strength=41.36 MPa and 0.127 mm thick) were used in diverse configurations considering thermal load by mismatch ($(\alpha_2-\alpha_1)\Delta T=-0.001$) in the case of dissimilar joints. According to the results, the adherent materials exhibit linear elastic behavior, whereas the material of the adhesive layer satisfies the elastic-perfectly plastic shear stress-strain constitutive relation.

The fatigue behavior of adhesive joints made with commercially coil-coated thin aluminum sheets (2 mm thick AA5754-O, Young modulus=68.9 GPa, Poisson ratio=0.33 and yield strength=165 MPa bonded with single-part, heat-cured rubber toughened adhesive (Young modulus=1.96 GPa, Poisson ratio=0.45 and yield strength=40 MPa was investigated by Datla et al [10]. In this work, double cantilever beam (DCB) and cracked lap shear (CLS) at 0° and 90° of rolling direction (different roughness) were employed. The results suggest, that the fatigue behavior was sensitive to the surface roughness introduced by the rolling lines (for example the CLS-Longitudinal specimens has an average value of fracture toughness of 181 J.m^{-1/2} until CLS-Transversal has 282 J.m^{-1/2}). Additionally, the presence of moisture in the test environment greatly reduced the fatigue threshold (25°C @ dry air: 145 J.m^{-1/2}, 40°C @ 100% RH: 57 J.m^{-1/2}). The employment of hybrid (adhesive-bolt or weld) joints were investigated by several researchers [11, 12, 13, 14, 15]. However, according to Wahab [4], the benefit to the fatigue performance of an adhesively bonded joint by additional bolting, riveting, or welding is questionable.

Recently, the behavior of multi-material structural adhesives has been studied for civil, automotive and aerospace applications. In that sense, Galvez et al [16], presented a study of the behavior of adhesive joints of steel with carbon fiber reinforced polymers (CFRP) for its application in bus structures. Such study presents a finite element model (FEM) of a bus steel, in order to obtain the forces that work on the reference node. Additionally, lap shear testing specimens were carried out; those specimens were made of CFRP-steel bonded with SikaTack Drive adhesive (polyurethane based). The results suggest, that the raised adhesive joint shows values far superior to the stresses that it must resist, greater elasticity at the reference node, decreasing the relative rigidity of the surroundings and minimizing mechanical fatigue.

The objective of the present paper is to analyze the influence of the adhesive and overlap length in the quasi-static fracture behavior and the dynamic loading response. The adhesive joints are composed of 6 mm thick anodized 6061-T6 aluminum alloy bonded to a 3 mm thick Dual Phase (DP) steel. Three different adhesives, with significant differences in mechanical properties were employed like Lord DC-80, Betamate 120 and MP55420. Extensometers were adhered in the joint center-line in order to measure strains generated during fatigue testing and validate if adherents are within the linear range. Overlap lengths of 12.7 and 50 mm were used in the experiment and 30, 50 and 70% of the maximum load were applied to the joint at R=0.1 and 30 Hz of frequency for fatigue tests. In order to predict fatigue life, maximum load-number of cycles Basquin and Wholer curves were built. Finally, scanning electron microscopy fractographs were taken upon the fracture surfaces, thus determine fractographic differences between adhesives.

MATERIALS AND METHODS

Two substrates have been used to prepare the single lap shear specimens: Anodized 6061-T6 aluminum plate (with dimensions of 1500×1500×6.4 mm), and DUAL-TEN® 590/600 (1500×1500×2.9 mm), a dual phase steel (ferrite matrix and approx. 5-15% martensite). Three different adhesives were used: one-component structural epoxy (Betamate 120), a two-component epoxy system (DC-80) and, a two component methyl methacrylate (MP55420). The Betamate 120 adhesive, is a one component epoxy paste adhesive with aluminum as filler, density of 1.14 g cm⁻³ and viscosity of 50 Pa s. The DC-80 adhesive, is a two components adhesive that consist of resin and hardener. The resin (density of 1.21 g cm⁻³ at 25 °C) is a paste that consists of 90 to 95% epoxy resin, 1 to 5% titanium dioxide, and 0.1 to 0.9% glass oxide. Moreover, the hardener (density of 1.01 g cm⁻³ at 25 °C) consists of 85 to 90% polyamide resin, 1 to 5% amine compound, 0.1 to 0.9% glass oxide and 0.1 to 0.9% epoxy resin. Finally, the MP55420 is a two-component methacrylate adhesive, consisting of resin and activator, with viscosities of 130 and 50 Pa s at 25 °C, respectively.

Adhesive Mechanical Characterization

Since that tensile properties may vary with rate and environment of testing, bulk adhesive specimens were prepared by following recommendations and agreement with adhesive manufacturer (see Fig. 1a). The procedure was as follow: first, the adhesive was poured within a polytetrafluoroethylene (Teflon®) mold (see Fig. 1b). The mold (8 mm thick) has three dog bone figures within, which dimensions are 16 mm, 6 mm thick, 38 mm of overall length, 12 mm of radius and gripping end of 28x50 mm. After pouring, the adhesives were subjected to the curing conditions that were specified by manufacturer instructions. The MP55420 adhesive (after mixed with the accelerator resin), generates an exothermic reaction that passes from 25 to 80 °C, then it reached its handling time after 5 min and finally full cure after 20 min. In the case of DC-80 adhesive, it was cured at 150 °C (in an oven) curing in 30 min. Finally, the Betamate 120 adhesive was submitted to 170 °C (in an oven) curing in 20 min.

Once curing was completed, the adhesive specimens could stand within the mold for 24 h. After curing schedule, the test specimens were tested following the procedure stated in ASTM D638 [17] by using a universal testing machine MTS810 equipped with a 100 kN load cell and flax knurled grips. The rate of testing was settled according adhesive manufacturer specifications (10 mm·min⁻¹). The tests were performed at room temperature (23 ± 1 °C). The transverse and longitudinal strain was measured by using a MTS Model AVX 54 advantage (class A) video extensometer that followed the width and gauge section (as depicted in Fig. 1) of test specimens during testing. The mechanical testing revealed the tensile strength, elongation and elastic properties (Young modulus and Poisson ratio) of every adhesive. In addition, stress and strain graphs were deployed from extensometer data and useful to sort adhesive depending on their mechanical behavior.

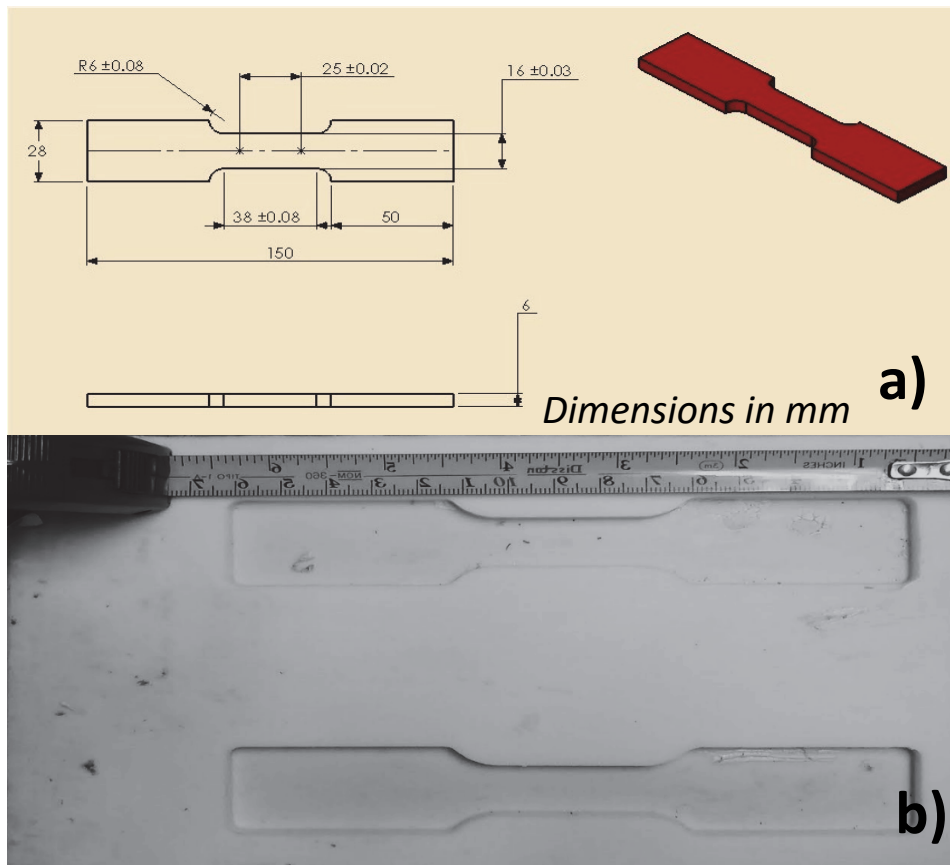


Figure 1: Tensile test specimen: a) general dimensions and b) Teflon® mold used in tensile test manufacturing.

Single lap shear (SLS) coupon and specimen manufactured.

The SLS specimens, were prepared by following procedure ASTM D1002 [18] by first preparing the test coupons. Before bonding, the adherend surfaces for aluminum (180 × 220 × 6.4 mm) and steel (180×220×2.9 mm) were cleaned with acetone, followed by an ultrasonic cleaning at 20 kHz for 30 min and dried with air (10 °C), finally wiped with acetone. The average roughness (R_a) for the cleaned steel and anodized aluminum adherends was 0.30 and 0.40 μm, respectively.

The surface energy was 48.32 and 53.02 J.m⁻² for cleaned steel and anodized aluminum, respectively. After the substrate surface finishing was completed, the adherents were bonded and cured considering 12.7 and 50.0 mm overlap length. Bond-line thickness is one of the important factors in adhesive joint because a thin bond-line is preferred over a thick one. The above due to the stress concentration at the corners of the joint is lesser in a thinner bond-line. In order to control bond-line thickness, glass beads (diameter of 0.180 mm) were added by manufacturer for MP55420 and Betamate 120 adhesives. On the contrary, metallic shims (0.180 mm in thickness) were positioned along the test coupon for the DC-80 adhesive.

After curing, test coupons were sawed and then machined until the specimen final dimensions were reached (25.4×101.6×adherend thickness in mm) and thicknesses of adhesive layer were measured (by means of an optical comparator) and the average was determined (0.180 mm). Five specimens were prepared in order to fulfill aforementioned standard. Tab. 1 summarizes the configurations in this experiment.

Overlap length (mm)	Adhesive	Adherend 1 Thickness (mm)	Adherend 2 Thickness (mm)
12.70	DC-80	AA6061 T6, 6.4 mm	Dual phase steel, 2.90 mm
	Betamate 120		
	MP55420		
50.00	DC-80	AA6061 T6, 6.4 mm	Dual phase steel, 2.90 mm
	Betamate 120		
	MP55420		

Table 1: Configurations used in this experiment.

Fig. 2 shows coupon and specimen used for this study. As can be noted, Fig. 2 depicts the original plate configuration (before bonding and after cleaning procedure), in such the testing coupon after curing where test specimens were outlined before cutting. Finally, the Fig. 2 red inset depicts the standard test specimen for single lap shear according to ASTM D1002 [18].

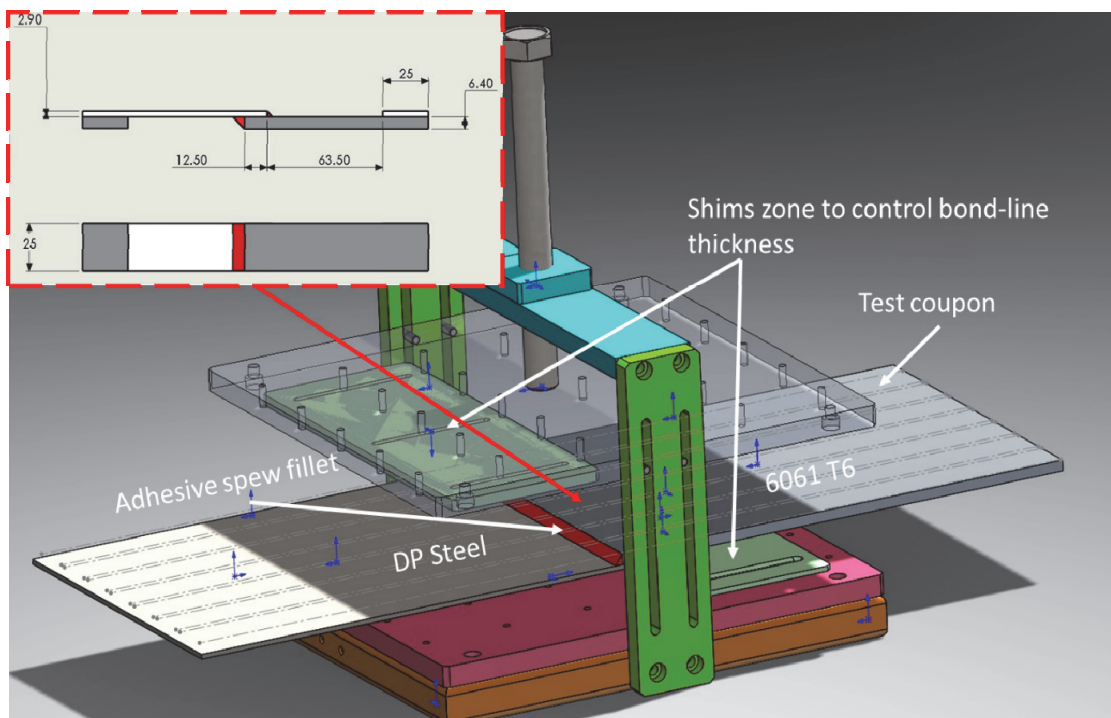


Figure 2: Test coupon adhesive bonding fixture and ASTM D1002 [18] test specimen.

Mechanical testing of Single lap shear (SLS) tests with 12.7 and 50.0 mm of overlap specimens

Before fatigue testing under the standard ASTM D3166–99 [19] it is necessary to know the maximum tensile load to set the parameters. The procedures used for testing the adhesive bonded joint were according the standard ASTM D1002 [18]. Rectangular tabs (25.4×6.4 or 2.9 mm) were bonded on the specimen extremes to assure an axial loading during testing. An INSTRON 4482 testing machine with flat knurled grips was used for the specimen testing. The rate of testing (2.4 kN min⁻¹ or approximately 1.2 mm·min⁻¹) was settled according to the standard ASTM D1002 [18]. It is known that polymeric materials may be rate sensitive, in this case, tests were carried out at temperatures below glass transition temperature (T_g) where rate sensitivity is negligible [20]. Additionally, foil strain gauges (Vishay EP-08-250BG-120) were bonded to the surface following the work of Karachalios et al [21].

The bond (adherend-strain gauges) remained for 24 h, and then the connecting cables were soldered to the extensometer terminals and connected to a P3 strain system. Then, SLS specimens, were tested in fatigue following ASTM D3166-99(2012) [19] procedures. An MTS 810 with flat knurled grips machine was used. The parameters were 0.1 of reversibility load ratio (R) and 30 Hz of frequency at 30, 50 and 70 % of the maximum load obtained in the SLS test. Both, 12.7 and 50.0 overlap length specimens were tested to build the S-N graphs. In this case, load-cycle graphs were built according to Ashcroft [22] and ten specimens were tested until they fractured or reaches 10⁶ cycles.

Post Fracture Analysis

After single lap shear and fatigue test, a visual inspection was performed on each fractured specimen to determine the fracture mode. An Optima V20 stereoscope was used to observe the fractured surfaces at magnification of 20x. Post fracture analysis was performed to complement the visual inspection, for the determination of the fracture mode upon the remaining adhesive on the surface. Post fracture analysis was performed with a JEOL LV600 scanning electron microscope operated at 15 kV with secondary electrons signal and working distance range was from 9 to 11 mm. The magnifications used were range from 100 x, 1000 x and 10000 x.

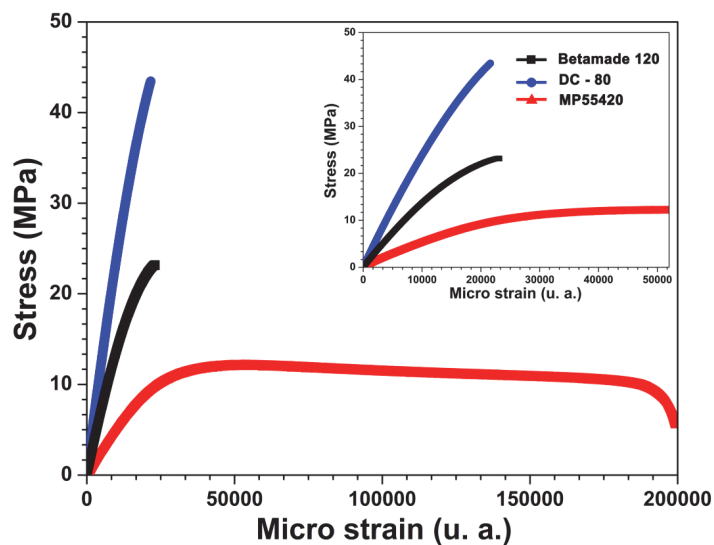


Figure 3: Stress-strain graphs for the DC-80, Betamate 120 and MP5520 adhesives.

RESULTS

Adhesive mechanical properties

Figure 3 which is a stress-strain chart depicts the relationships between these for every adhesive. It means, that each adhesive could behave (deform) different when is subjected to an external stress. The DC-80 adhesive (blue dashed graph in Fig. 3) has a tensile strength of 43.44 ± 0.88 MPa, $1.8 \pm 0.3\%$ of elongation, a Poisson ratio 0.336 and a Young modulus of 2383 ± 54 MPa. On the other hand, the Betamate 120 adhesive (red dashed graph in Fig. 3), had a tensile strength of 23.24 ± 0.50 MPa, $2.3 \pm 0.02\%$ of elongation, a Poisson ratio 0.292 and a Young modulus of 1371.8 ± 23.4 MPa. Finally, the MP55420 adhesive (black continuous lined graph in Fig. 3), had a tensile strength of 12.00 ± 0.25 MPa, $20.3 \pm 0.45\%$ of elongation, a Poisson ratio 0.305 and a Young modulus of 471.55 ± 4.88 MPa. The results were similar to

those reported by Cruz et al [23]. Finally, according to Akhavan et al [24], the MPP5420 adhesive falls within the very ductile adhesive classification while the other two in the intermediate strength classification.

As can be noted from Fig. 3, the mechanical behavior was different among the three adhesives even at first sight. The stress-strain graph for the DC-80 adhesive, reveals a straight line and small area under it, whereas the Betamate 120 depict a small transition between elastic-plastic behaviors but without significant difference between elongation values. In contrast, the MP55420 showed a transition between elastic-plastic behaviors, however its elongation was higher in comparison to the other two adhesives. The highest slope (expressed as Young modulus) was depicted by DC-80 adhesive and its Young Modulus is almost twice the Betamate 120 modulus and five times higher than MP5520 modulus.

Single lap shear testing results

The results, expressed as load-displacement graph, are depicted in the Fig. 4. The SLS for the 12.7 mm overlap length DC-80 joint was 5980 ± 320 N, 5743 ± 130 N for the 12.7mm overlap length Betamate 120 adhesive joint and 4269 ± 280 N for the 12.7mm overlap length MP55420 adhesive joint. On the other hand, the 50.0 mm overlap length joint made with Betamate 120 adhesive revealed a SLS of 20980 ± 320 N (3.50 higher than the 12.7 mm), in the case of the 50.0 overlap length joint made with DC-80 adhesive revealed a SLS of 17911 ± 570 N (3.12 higher than the 12.7 mm) and finally 9250 ± 176 N (2.20 higher than the 12.7 mm) for MP55420 joint.

The displacement was 0.65 mm for the 12.7 mm overlap length group of adhesives, contrasting a 1.2 to 1.8 mm for the case of the 50.0 mm group. It worth mention, that the highest displacement was noted for the Betamate 120 adhesive, followed by the DC-80 adhesive and finally the MP55420. The DC-80 adhesive, reveals a broken glass like sound before break approximately at 60% of the maximum load. The MP55420, reveal some striations upon the spew fillet at 50% of its maximum load, because its ductility is higher than the other two adhesives. The 50.0 mm overlap group reveals some bending in the adherents being more pronounced in the steel side at approximately 80% of their maximum load.

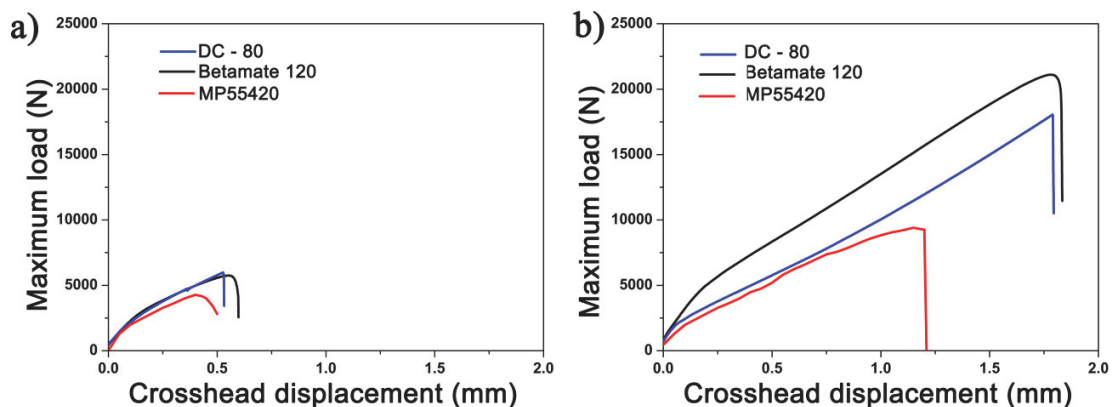


Figure 4: Load-displacement derived from SLS testing for: a) 12.7mm overlap length and b) 50.0 mm overlap length.

The strain measurement revealed that the HSLA steel reached a maximum micro-strain of -300×10^{-6} and -508×10^{-6} at maximum load for 12.7 and 50.0 mm of overlap respectively, then according to Hooke law the stress at this point is below its yield stress. However, in the case of aluminum the higher strains were noted (see Tab. 2), however the Betamate 120 reaches a strain near to the aluminum yield stress (the value was 233 MPa in comparison to the aluminum yield stress of 250 MPa) at 90% of its maximum load. The above, suggests that maximum strain was withstand by the adhesive itself, since its mechanical properties are small in comparison to the adherends.

After mechanical characterization, loads for the fatigue testing were selected according to ASTM procedures (50 % of the maximum shear load as initial) and some spectra to analyze the fatigue behavior in loads higher than 50 % and loads lesser than 50 %. However, for Betamate 120 adhesive, loads near to 90 % of its maximum could generate yielding and bending would act as stress riser. In that sense, 70 % of its maximum was selected and finally 30 % of the maximum load in order to obtain a point of comparison in a wide range of loading.

Fatigue results

Fatigue testing results are presented in Figs. 5, 6 and 7. Fig. 5 shows the S-N curves for a bonding with DC-80 adhesive for both 12.7 and 50 mm overlapping. Fig. 6 depicts the S-N curves for bonding with Betamate 120 for both 12.7 and 50



mm overlapping. The S-N curves for bonding with MM55420 for both 12.7 and 50 mm overlapping are also shown in Fig. 7. As usual, the higher overlapping increases the cyclic maximum load achieved at 10^6 cycles. The maximum fatigue loading for DC80 adhesive at 10^6 cycles is 1.75 kN for overlapping 12.7 mm and 4.8 kN for overlapping 50 mm. For Betamate 120 adhesive maximum fatigue loading at 10^6 cycles is 1.8 kN for 12.7 and of overlapping and 6 kN for 50 mm of overlapping. Finally, for MP55420 the maximum fatigue loading at 10^6 cycles is 1.3 kN for an overlapping of 12.7 mm and 2.9 kN for 50 mm of overlapping. In general terms for an overlapping of 12.7 mm the fatigue behavior is better when the joint is adhered with Betamate 120 but slightly higher than DC 80. When the joint is adhered with an overlapping of 50 mm, Betamate exhibits the best dynamic behavior. Fatigue results were obtained by using 15 specimens per overlapping and per adhesive. The data were statistically treated to get fatigue models such as Whöler or Basquin by using regressions. Tab. 3 shows the coefficients for such models for each adhesive.

Overlap (mm)	Load (N)	Strain $\times 10^{-6}$	% of Maximum Load	Overlap (mm)	Load (N)	Strain $\times 10^{-6}$	% of Maximum Load	
12.7	DC-80	500	320	8.36	DC-80	1000	120	5.58
		1000	579	16.72		3000	340	16.75
		2000	1000	33.44		6000	1000	33.50
		3000	1280	50.17		9000	2108	50.25
		4000	1780	66.89		12000	2380	67.00
	Betamate 120	5000	2160	83.61	16000	2590	89.33	
		500	588	8.71	1000	588	4.77	
		1000	780	17.41	4000	1000	19.07	
		2000	1250	34.83	8000	1480	38.13	
		3000	1377	52.24	12000	2000	57.20	
MP55420	4000	1800	69.65	16000	2800	76.26		
	5000	2345	87.06	19000	3380	90.56		
	500	200	11.71	500	320	5.41		
	1000	540	23.42	1000	654	10.81		
	2000	800	46.85	2000	1000	21.62		
MP55420	3000	1050	70.27	6000	1680	64.86		
	4000	1280	93.70	8000	1560	86.49		

Table 2: Strain gauge measurements results at different load for the three adhesives with 12.7 and 50.0 mm overlap length.

On the other hand, it is important to compare the maximum load achieved under dynamic loading versus quasi-static loading. For DC-80 the load resisted in fatigue (10^6 cycles) represents 27 % of the maximum static loading for both 12.7 and 50 mm overlapping. For Betamate 120 the maximum loading resisting fatigue is 28 % of the maximum static loading reached. Finally, for MP55420, exhibiting the worst static and dynamic maximum load resistance, the fatigue load achieved is 25% of the maximum static strength for 12.7 mm and 31% for 50 mm overlapping. According to the results, of course a bigger overlapping is better, but Betamate 120 exhibits the best behavior when solicited statically and dynamically too.

Post fracture analysis

The visual inspection results are depicted in Figs. 8a), 8b) and 8c). The DC-80 adhesive test specimen revealed cohesive-adhesive failure where 60 % of the adhesive remained on the aluminum side (see Fig. 8a). On the contrary, Betamate 120

adhesive (Fig. 8b) and MP55420 adhesive test specimens (Fig. 8c) reached a 100 % cohesive failure. It means that for latters, the crack ran through the adhesive bond-line. On the other hand, the DC-80 test specimens showed that the crack ran through the adhesive bond-line and it's interface. As can be noted from Fig. 8a), the adhesive spew fillets remained upon the surface, suggesting that it was the crack origin. Since, the edge of the lap joint was the higher stress zone, a fractographic analysis with scanning electron microscope was conducted.

Overlap (mm)		Whöler model $\text{Log } N_f = A \cdot S_a + B$			Basquin model $\text{Log } N_f = A \cdot \text{Log } S_a + B$		
		A	B	Std Dev	A	B	Std Dev
12.7	DC80	-1.0716	7.4349	0.976	-7.019	7.3927	0.1513
50.0		-0.3534	7.6551	2.926	-5.887	10.366	0.1511
12.7	Betamate 120	-0.5743	6.7718	0.9377	-3.695	6.7221	0.1527
50.0		-0.1802	7.129	3.443	-3.942	9.1617	0.1526
12.7	MP55420	-1.3595	7.7687	0.6968	-5.905	6.6818	0.1523
50.0		-0.4350	7.7293	1.5101	-4.253	7.9596	0.1512

Table 3: Coefficient of Whöler and Basquin models for adhesive joints in fatigue (S [kN]).

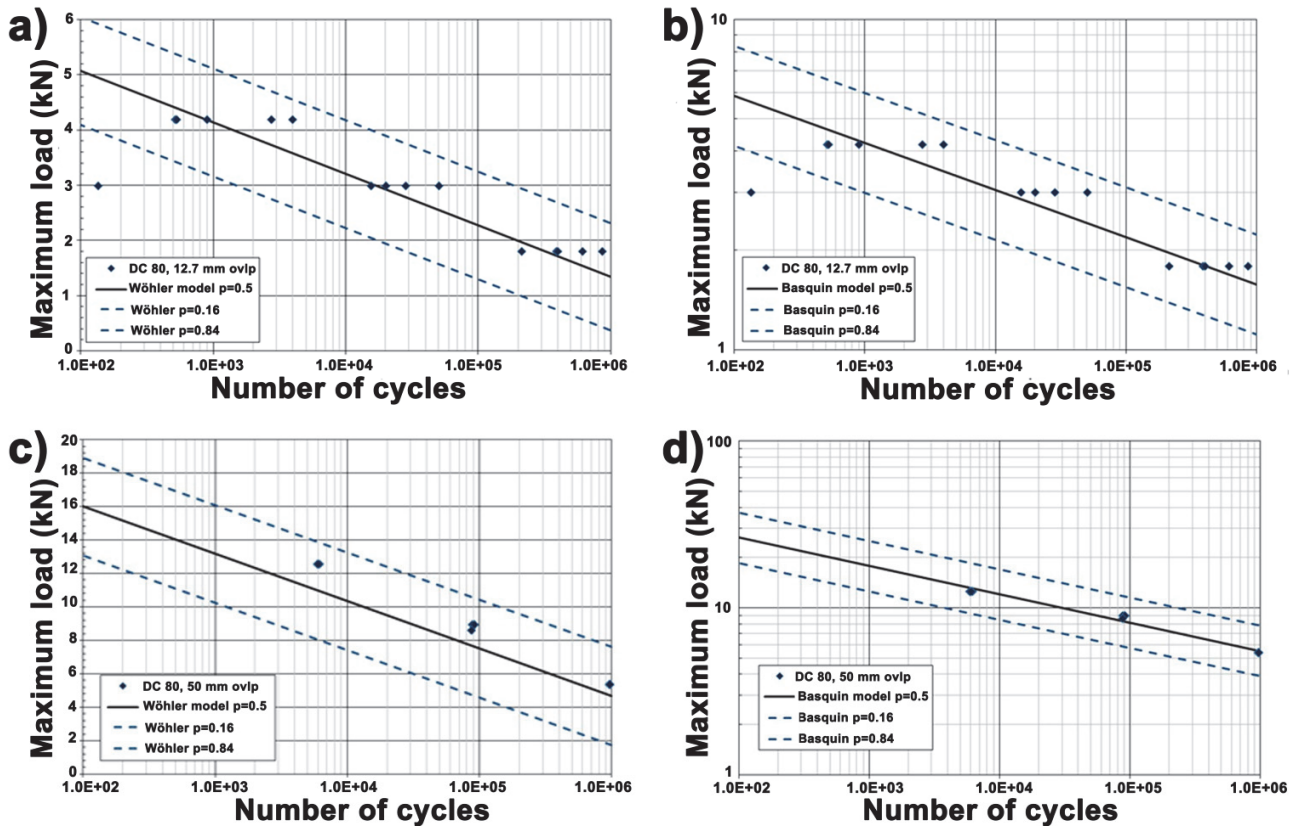


Figure 5: a) and b) 6061-T6 DC-80 adhesive bonded joint with 12.7 mm overlap length Whöler and Basquin graphs, c) and d) Whöler and Basquin graphs for 6061-T6 DC-80 adhesive bonded joint with 50.0 mm.

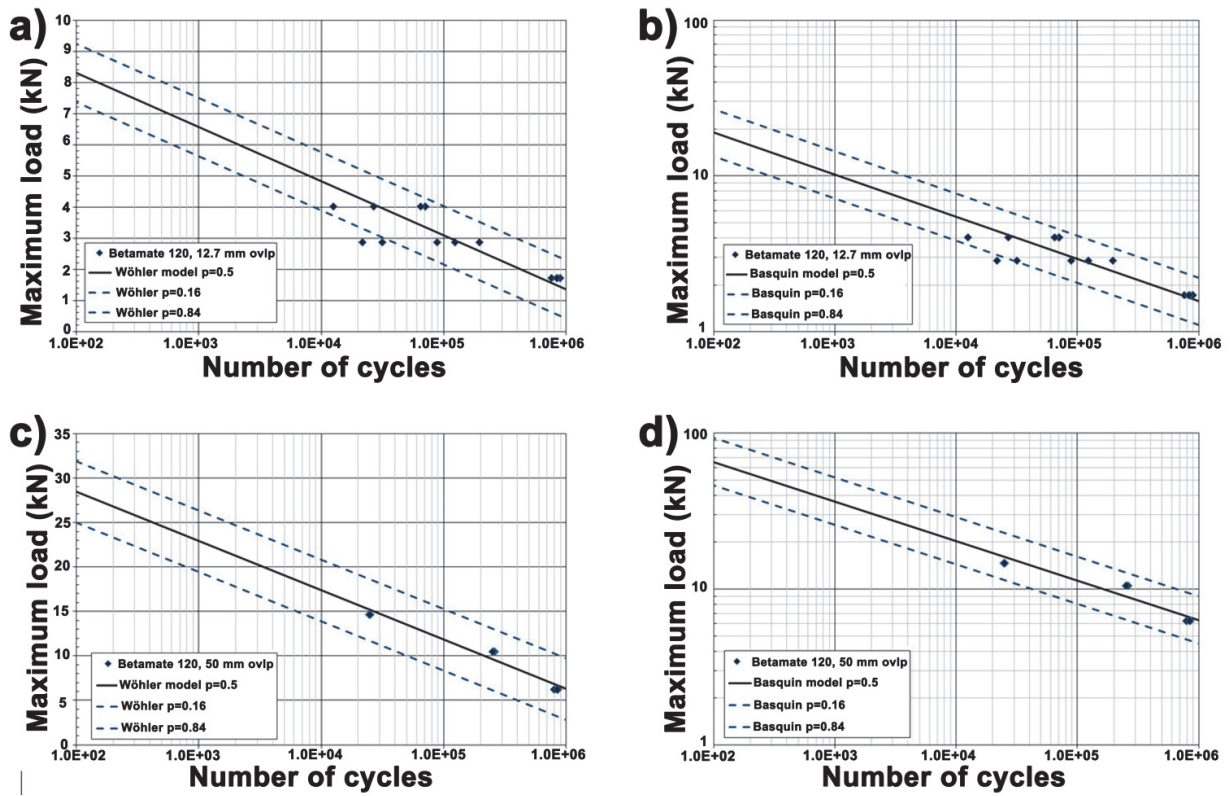


Figure 6: a) and b) 6061-T6 Betamate 120 adhesive bonded joint with 12.7 mm overlap length Wholer and Basquin graphs, c) and d) Wholer and Basquin graphs for 6061-T6 Betamate 120 adhesive bonded joint with 50.0 mm (down).

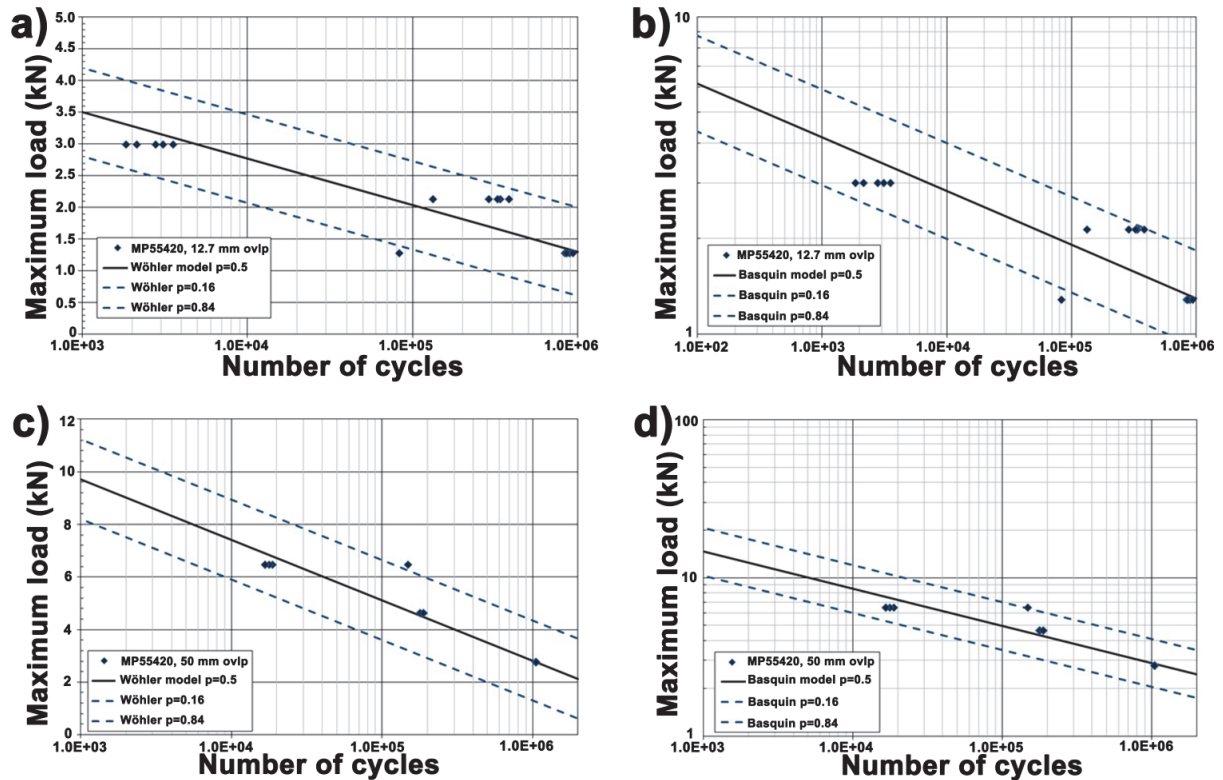


Figure 7: a) and b) 6061-T6 MP55420 adhesive bonded joint with 12.7 mm overlap length Wholer and Basquin graphs, c) and d) Wholer and Basquin graphs for AA6061-T6 MP55420 adhesive bonded joint with 50.0 mm.

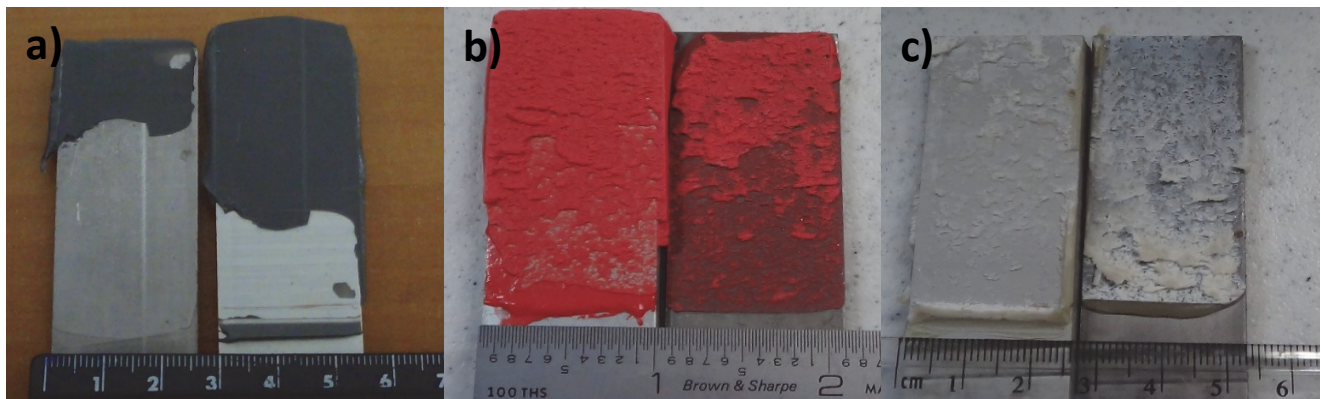


Figure 8: Visual inspection of: a) DC-80, b) Betamate 120 and c) MP55420 test specimens.

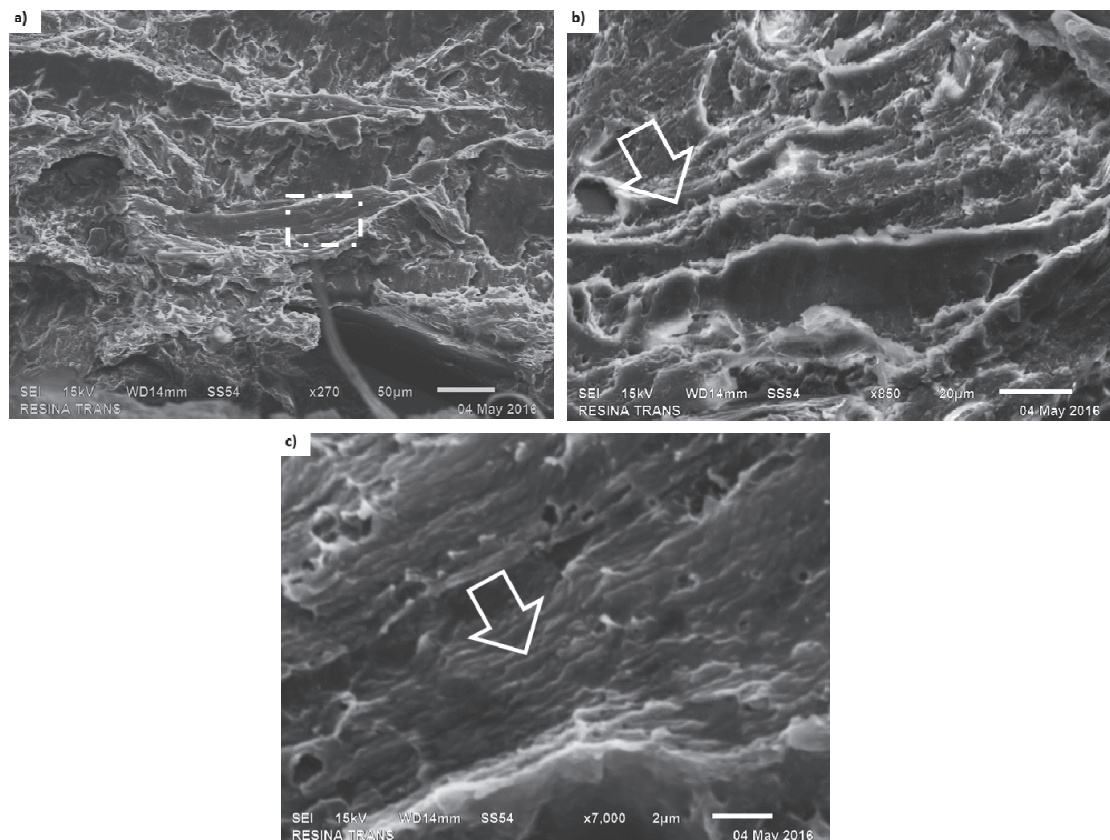


Figure 9: SEM fractographs of fatigue fractured single-lap shear specimens with overlap length of 50 mm containing MP55420 adhesive at fillet zone: a) rough surface, b) apparent striations, and c) resolved fatigue striations.

The fractographic analysis from the fractured surfaces at the spew fillet area near steel side of single-lap shear specimens under fatigue with 70 % of maximum load and overlap length of 50 mm (higher shear loads and displacements than that of 12.7 mm group) containing MP55420 adhesive (Fig. 9) exhibited rough surfaces with fatigue fracture appearance within the adhesive (Fig. 9a) that exhibited lower cohesive strength [25]. At major magnification, it can be observed apparent and discontinuous fatigue striations, (see Fig. 9b), which were confirmed with larger amplification finding several short resolved fatigue striations, as can be presented in Fig. 9c). This features fatigue behavior could be favored with the application of 70 % of maximum fatigue load that reduced the test time, indicating that the fatigue mechanism would be decreased. Moreover, the extended plastic strain behaviour with the biggest elongation and lowest tensile strength, i.e., the

highest ductility reached by the MP55420 adhesive lap joint (see red inset in Fig. 3) and the lowest fatigue loading at 10^6 cycles (Fig. 7) compared to that of other adhesives, clearly confirmed the described fatigue fracture.

Fig. 10 showed the fatigue fractured surfaces of Betamate 120 adhesive at fillet zone near steel side from single-lap shear specimens with overlap length of 50 mm for 70 % of applied maximum load, which exhibited fatigue fracture area with less rough surface containing several nearly rounded particles and micro-dimples (Fig. 10a). At bigger amplification, a nearly flat surface could be seen in Fig. 10b), and a clearly flat surface containing well resolved striations and small particles is observed in Fig. 10c). Besides, it was observed several small semi-rounded metallic particles within fatigue fractured surfaces linked to the composition of the adhesive with aluminum as filler. The Betamate 120 adhesive used in fatigue specimens reached a fatigue behavior that was linked to the moderated elastic deformation and Young modulus, limited tensile strength and the highest fatigue loading at 10^6 cycles (Fig. 6) compared to that of DC-80 and MP55420 adhesives. Therefore, single-lap shear specimens with Betamate 120 adhesive reached the best dynamic behavior under fatigue.

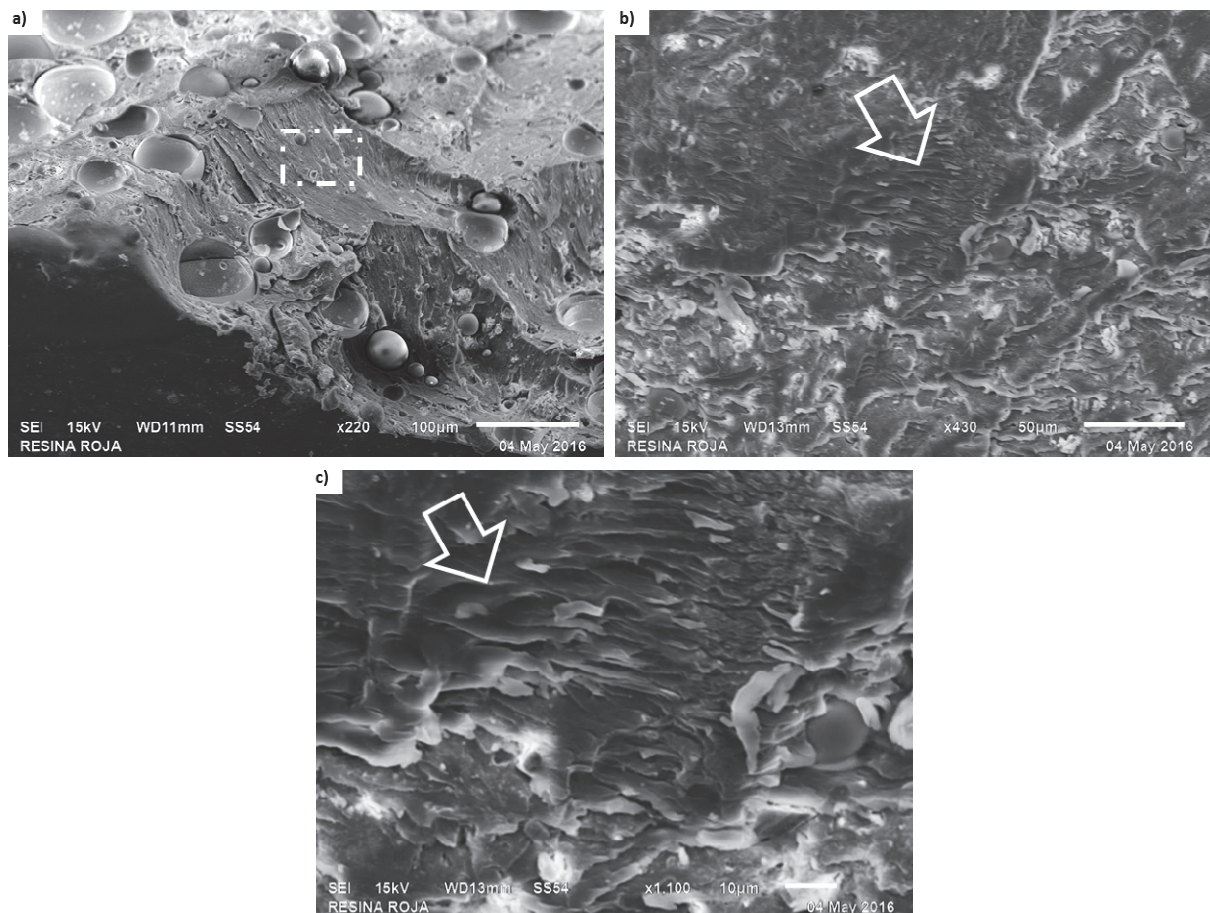


Figure 10: SEM fractographs of fatigue fractured single-lap shear specimens with overlap length of 50 mm containing Betamate 120 adhesive at fillet zone: a) less rough fracture with several particles, b) nearly flat surface, and c) resolved fatigue striations.

For the fatigue fractured surfaces at the DC-80 adhesive at fillet area near steel side from single-lap shear specimens with overlap length of 50 mm and 70 % of applied maximum load (Fig. 11), it's clearly observed a brittle failure [25, 26] with interesting features, i.e., flat surfaces of variable extension (Fig. 11a), well-defined flat quasi-cleavage facets containing notable river patterns in the direction of fatigue crack propagation (Fig. 11b), which were observed at major magnification in Fig. 11c). Moreover, the fatigue fractured specimens joined by DC-80 adhesive exhibited notable facet fragile failure that was confirmed by the shape of stress-strain plot with straight line from the origin to the point of fracture [25], completely elastic strain behaviour without plastic deformation, the highest tensile strength and abruptly fracture, as can be seen in the curve of Fig. 3.

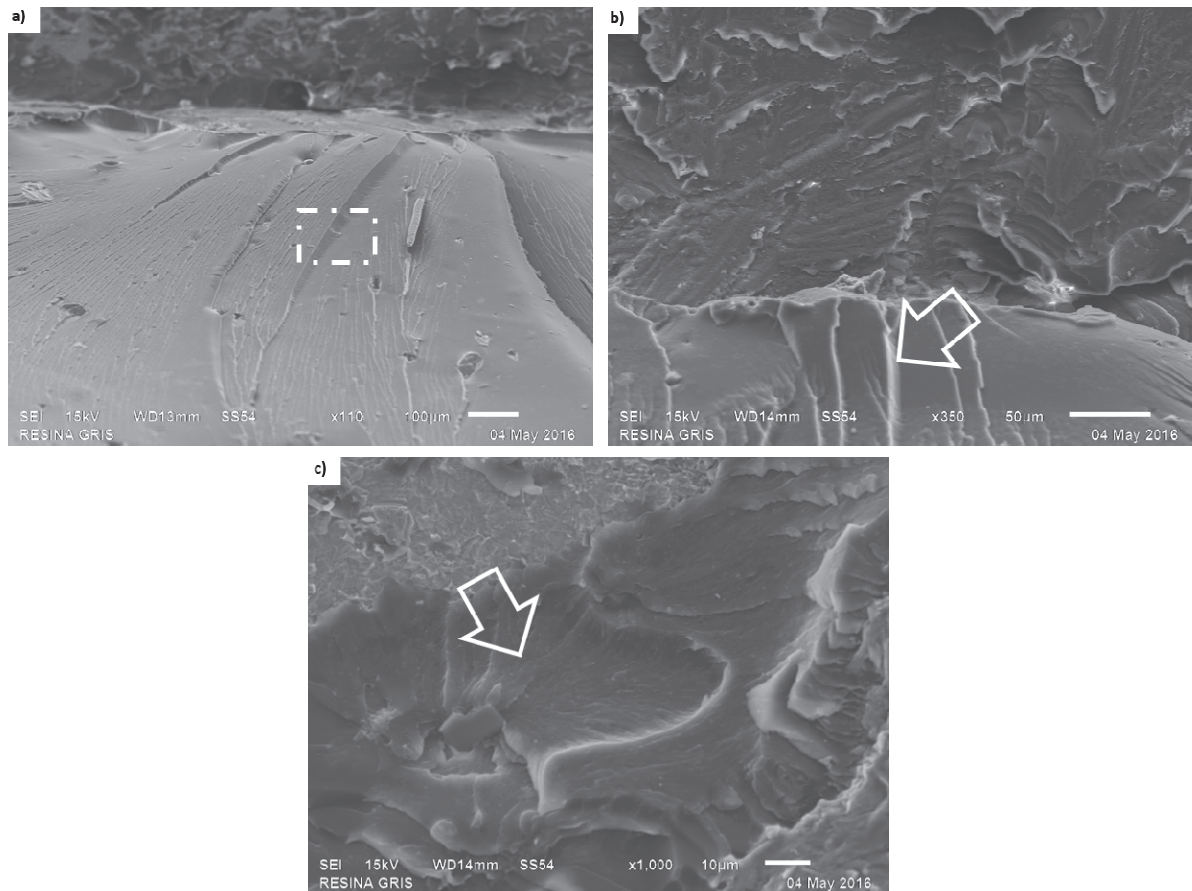


Figure 11: SEM fractographs of fatigue fractured single-lap shear specimens with overlap length of 50 mm containing DC-80 adhesive at fillet zone: a) quasi-cleavage brittle failure, b) well-defined river patterns on facets, and c) facets at major magnification.

Discussion

The static tensile tests, for the bulk adhesives revealed that the adhesives ranged to a low strength one to a higher strength one. The MP55420 adhesive had lower strength and higher ductility, its elastic properties suggested that it yield at lower normal loads in comparison to the Betamate 120 and DC-80 adhesives. In addition, MP55420 adhesive could sustain higher strains in contrast to the other two adhesives. However, MP55420 had lower strength in comparison to the other two adhesives. Typically, in lap shear joints there are two components of stress: shear (τ) and normal (σ_y) stresses. Since that MP55420 failed first since its lower strength, for that reason the strain in the adherents was lower in comparison to the other adhesives.

In balanced joints (same thickness and material), the normal stress occurred because an eccentricity was generated during specimen loading. Additionally, failure predictions for balanced joints were proposed by Karachalios et al [20] suggesting that for the short overlaps, failure was dominated by global yielding in the adhesive layer. If the adhesive is ductile, then this method of prediction could probably be valid for longer overlaps too. However, if the adhesive is brittle, global yielding as a failure criterion would only be applicable for short overlaps. Similar trend was reported by Banea et al [27], for the case of multi-material joints (high strength steel and carbon fiber reinforced plastics-Aluminum). However, Shiu [28] results suggested that for dissimilar adherends, the maximum shear stress occurs at the free end of adhesive region near to the adherend with higher stiffness.

A difference in displacements was noted, since that the brittle adhesives seem to sustain a higher displacement in comparison to ductile one. In that sense, Banea et al [27] reported for multi-material joints that geometrical balanced joints (approximately same thickness) promoted higher strength than that of the stiffness balanced joints (thickness of one adherend was approximately twice the other) because large rotation and displacements are promoted. For example, within



Baneas' work for the CFRP (Carbon Fiber Reinforced Polymer) 50.0 mm length overlap joint yield a displacement of 6.0 mm. However, with the same overlap length, both geometrically and stiffness balanced joints yielded a displacement of 5.0 mm. The same trend was noted for the 12.5 mm length overlap.

In that sense and considering that the adherents exhibited linear elastic behavior, SLS specimens started their failure at the steel side by global yielding (12.7 mm overlap length) and since they had a similar failure mode, their displacement was similar, not so their strength since it would depend on the adhesive mechanical properties. However, a slightly difference was noted for long overlaps as 50 mm, it may be produced by a difference in the failure mode like the fatigue (Betamate 120 and MP55420 adhesives) and brittle fracture for DC80 adhesive joints, because in the case of ductile adhesives like MP55420 and Betamate 120, the joint would fail with global yielding. Therefore, the best adhesive joint in terms of dynamic fatigue behavior was the single-lap shear specimens with Betamate 120 adhesive for overlap length of 50 mm under 70 % of applied maximum load, which exhibited fracture containing nearly flat surfaces containing well resolved striations at the highest fatigue loading (6 kN) at 10^6 cycles.

It is important to note that fatigue in adhesive joints was present and not only quasi-static fracture can be expected, but cyclic damage can occur if dynamic loads were applied. Fracture surface of specimens failed in fatigue showed characteristics such as striations, river patterns in the crack propagation direction and particle displacements linked to a dynamic load response, confirming the probability to experience a fracture below the maximum static strength as reported [3, 4]. The fatigue behavior observed in these adhesive joints was consistent and the scatter was moderate. The fracture surfaces showed differences, however all the adhesives studied experience fatigue damage micro-features that must be considered in addition to the mechanical characteristics when used in industrial designs.

CONCLUSIONS

The fatigue strength and fracture behavior for a dual phase steel-AA6061-T6 bonded joints with three different adhesives (DC-80, Betamate 120 and MP55420) was analyzed. Previously, single lap shear tests were carried out to determine maximum shear loads, for 50 mm overlap length results that were 2 to 3.5 times higher in comparison to the 12.7 mm overlap length specimens. The results for the strain measurement revealed that the higher strain-stress were developed in the 6061-T6 aluminum alloy adherend and in all cases they were lower than the adherends yield strength.

Fatigue testing were carried out on five specimen sets at 30, 50 and 70 % of the maximum shear load, 0.1 of reversibility load ratio (R) and 30 Hz of frequency. After testing, Basquin and Wholer graphs were built for each adhesive at 12.7 and 50.0 mm of overlap length. The results suggested that at higher overlapping, the cyclic maximum load increased. Additionally, for 12.7 and 50.0 mm of overlapping, the maximum fatigue loading at 10^6 cycles for Betamate 120 adhesive was 1.8 and 6 kN respectively; followed by the DC80 adhesive with 1.75 and 4.8 kN; finally the MP55420 adhesive reached 1.3 and 2.9 kN.

The post-fracture analysis revealed that MP55420 and Betamate 120 adhesives had a cohesive failure, while the DC-80 showed cohesive-adhesive fracture. Additionally, the scanning electron microscopy study on the spew fillet exhibited resolved striations and a network of small micro-dimples for the Betamate 120 and MP55420 adhesives. On the contrary, DC-80 adhesive showed notable facet fragile failure that was confirmed by the shape of stress-strain plot with straight line from the origin until fracture.

REFERENCES

- [1] Cruz Gonzalez, C., Gonzalez-Garcia, P., Santillan-Gutierrez, S., Taha-Tijerina, J. and R. Romero-Llerenas, (2017). Scanning electron microscopy, atomic force microscopy and optical profilometry applied to adhesive bonding technologies, Microscopy and imaging science: practical approaches to applied research and education, Badajoz, Mendes-Vilas. Formatex Research Center, pp. 464-473.
- [2] E. M. Petrie (2007). Handbook of Adhesives and Sealants., Chicago, Mc Graw-Hill,.
- [3] Jeandrau, J.-P., Peyrac, C., Lefebvre, F., Renard, J., Gantchenko, V., Patamaprohm, B. and Guinault, C. (2015). Fatigue behaviour of adhesive joints, 6th Fatigue Design conference, Fatigue Design 2015, Senlis, France.
- [4] Abdel Wahab, M., (2012). Fatigue in Adhesively Bonded Joints: A Review, International Scholarly Research Network, 12, pp. 1-25.



- [5] Bermejo, R., Oñoro, J. and García-Ledesma, R. (2008). Comportamiento a fatiga de uniones a solape simple con adhesivo epoxi de acero y acero prepintado, *Revista de Metalurgia*, 44 (4), pp. 310-316.
- [6] Altan, G., Topcu, M. and Callioglou, H. (2010). The effects of the butterfly joints on failure loads and fatigue performance of composite structures. *Science and Engineering of Composite Materials*, 17 (3), pp. 199–212.
- [7] Fessel, G., Broughton, J.G., Fellows, N.A., Durodola J.F. and Hutchinson, A. R. (2009). Fatigue performance of metallic reverse bent joints, *Fat Fract Eng Mat Struct.*, 32 (9), pp. 704–712.
- [8] Azari, S., Papini, M. and Spelt, J.K. (2011). Effect of adhesive thickness on fatigue and fracture of toughened epoxy joints – Part I: Experiments, *Eng Fract Mech*, 78 (1), pp. 153-162.
- [9] Markolefas, S.I. and Papathanassiou, T. (2009). Stress redistributions in adhesively bonded double-lap joints, with elastic–perfectly plastic adhesive behavior, subjected to axial lap-shear cyclic loading, *Int. J. of Adhesion & Adhesives*, 29 (7), pp. 737–744.
- [10] Datla, N.V., Papini, M., Schroeder, J.A. and Spelt, J.K. (2010). Modified DCB and CLS specimens for mixed-mode fatigue testing of adhesively bonded thin sheets, *Int. J. of Adhesion & Adhesives*, 30 (6), pp. 439–447.
- [11] Hoang-Ngoc, C.-T. and Paroissien, E. (2010). Simulation of single-lap bonded and hybrid (bolted/bonded) joints with flexible adhesive, *Int. J. of Adhesion and Adhesives*, 30 (3), pp. 117–129, 2010.
- [12] Kelly, G. (2006). Quasi-static strength and fatigue life of hybrid (bonded/bolted) composite single-lap joints, *Composite Structures*, 72 (1), pp. 119-129.
- [13] Sam, S. and Shome, M. (2010). Static and fatigue performance of weld bonded dual phase steel sheets, *Science and Technology of Welding & Joining*, 15 (3), pp. 242–247.
- [14] Goncalves, V.M. and Martins, P.A.F. (2006). Static and fatigue performance of weld-bonded stainless steel joints, *Materials and Manufacturing Processes*, 21 (8), pp. 774–778.
- [15] Chang, B.H., Shi, Y.W. and Lu, L.Q. (2001). Studies on the stress distribution and fatigue behavior of weld-bonded lap shear joints, *J. of Materials Processing Technology*, 108 (3), pp. 307-313, 2001.
- [16] Galvez, P., Quesada, A., Martinez, M. A., Abenojar, J., Boada, M.J.L. and Diaz, V. (2017). Study of the behaviour of adhesive joints of steel with CFRP for its application in bus structures, *Composites Part B*, 129, pp. 41-46.
- [17] ASTM D638 (2014). Standard Test Method for Tensile Properties of Plastics. ASTM International, West Conshohocken, PA, USA.
- [18] ASTM D1002 (2010). Standard Test Method for Apparent Shear Strength of Single-Lap-Joint Adhesively Bonded Metal Specimens by Tension Loading (Metal-to-Metal). ASTM International, West Conshohocken, PA, USA.
- [19] ASTM D3166-99 (2012). Standard Test Method for Fatigue Properties of Adhesives in Shear by Tension Loading (Metal/Metal). ASTM International, West Conshohocken, PA, USA.
- [20] Karachalios, E.F., Adams, R.D. and Silva, L. da (2013). The behaviour of single lap joints under bending loading," *J. of Adhesion Science and Technology*, 27 (16), pp. 1811–1827.
- [21] Karachalios, E.F., Adams, R.D. and Silva, L. da (2013). Single lap joints loaded in tension with ductile steel adherends, *Int. J. of Adhesion & Adhesives*, 43, pp. 96-108.
- [22] Ashcroft, I.A. (2005). *Adhesive Bonding - Science, Technology and Applications*, Chapter 10. Fatigue. Woodhead Publishing, pp. 209-239.
- [23] Cruz-Gonzalez, C., Jamilloux, A., Santillan-Gutierrez, S., Gonzalez-Garcia, P., Taha-Tijerina, J., Romero, R. and Gamez-Cuatzin, H. (2018). Evaluacion por elementos finitos de uniones con adhesivos de materiales disimiles (acero-aluminio), *Dyna. Ingeniería e Industria*, 4, pp. 404-410.
- [24] Akhavan-Safar, A., da Silva, L. and Ayatollahi, M. (2017). An investigation on the strength of single lap adhesive joints with a wide range of materials and dimensions using a critical distance approach, *Int. J. of Adhesion and Adhesives*, 78, pp. 248-255.
- [25] Becker, W.T. and Shipley, R.J. (2002). *ASM Handbook. Volume 11: Failure Analysis and Prevention*, ASM International, pp. 627-640.
- [26] Atif, R. and Inam, F. (2016). Influence of Macro-Topography on Damage Tolerance and Fracture Toughness of Monolithic Epoxy for Tribological Applications, *World Journal of Engineering and Technology*, 4 (2), pp. 335-360.
- [27] Banea, M. D., Rosioara, M., Carbas, R. and da Silva, L. (2018). Multi-material adhesive joints for automotive industry, *Composites Part B*, 151, p. 71–77.
- [28] Shiuh-Chuan, H. (1999). Stress analysis of adhesively-bonded lap joints, *Composite Structures*, 47, pp. 673-678.